**PAPER** • **OPEN ACCESS**

# Electrochemical corrosion performance of eutectic Al-Si automotive alloy in 0.1 M and 0.2 M NaCl solution

To cite this article: Akib Abdullah Khan and Mohammad Salim Kaiser 2022 *IOP Conf. Ser.: Mater. Sci. Eng.* **1248** 012031





# Electrochemical corrosion performance of eutectic Al-Si automotive alloy in 0.1 M and 0.2 M NaCl solution

**Akib Abdullah Khan[1] *, Mohammad Salim Kaiser[2]**

[1]Department of Mechanical Engineering, Bangladesh University of Engineering and Technology, Dhaka-1000, Bangladesh

[2]Directorate of Advisory, Extension and Research Services, Bangladesh University of Engineering and Technology, Dhaka-1000, Bangladesh

*Corresponding Author: E-mail: 1610170@me.buet.ac.bd; Tel.: +8801521432085;

**Abstract**. Corrosion behavior of eutectic Al-Si automotive alloy is investigated in different strengths of 0.1 M and 0.2 M NaCl solution at room temperature. Alloy with Si as trace impurity is also considered for the comparison of the property. The study is done by electrochemical method, using potentiodynamic polarization measurements and electrochemical impedance spectroscopy (EIS) techniques. The alloy surfaces are characterized by both optical microscopy and scanning electron microscopy. The results indicate that Si addition improves the corrosion performance of the Al-Si automotive alloy and this improvement is more pronounced in higher corrosive environments. The corrosion rate along with current density ($I_{corr}$) of trace Si added alloy showed higher value than that of higher Si added alloy. The corrosion potential ($E_{corr}$) and open circuit potential (OCP) of higher Si added alloy are shifted to the more noble direction. The cause behind this, the higher amount of $Mg_2Si$ precipitates in higher Si added alloys tends to form oxides like $SiO_2$ and MgO which protects the surfaces from further corrosion. Microscopic images confirm that the polishing scratches on the surfaces of the alloys are not visible after corrosion. The SEM images also confirm that the corroded surfaces seem to have pit formations which are lower in higher Si added alloys due to formation of a protective layer of oxides. The higher corrosion performance is observed for higher Si added alloys especially in higher strength of corrosive environment.

## 1. Introduction

Aluminium alloys are nowadays considered as a paramount material as they have good weight/strength ratio and high corrosion resistance. Aluminum alloys are utilized extensively in the aircraft, automobile, marine, and construction industries [1]. Several elements are added in certain quantities into the aluminium alloys to modify mechanical or corrosion properties [2]. Degradation or deterioration of metal is referred to as corrosion. Corrosion is electrochemical in nature and comprises two or more processes on the metal's surface. Two corrosion reactions are oxidation and reduction; oxidation is known as anodic partial reaction and reduction is known as cathodic partial reaction. Corrosion processes influence both the chemical and physical properties of an alloy [3]. Under the majority of accessible service conditions, aluminum alloys have shown to be highly resistant to corrosion [4]. This is owing to the fact that aluminium forms a thin protective layer of oxide that is tightly bound to surface materials [5]. When an aluminum alloy is immersed in a sodium chloride solution, the solution functions

as a corrosive medium that damages the material. As a result of chloride ions substituting oxygen ions in the oxide lattice, the passive films are weakened and thinning [6]. NaCl can get in contact with piston material in many ways. It can enter the fuel as sodium carriers [7]. Salt driers at the refinery or tankers that use sea water to flush their tanks, road salt, salt spray, and other means can also introduce sodium chloride into the fuel [8]. Besides, in marine applications, engine materials or other materials of the ships get into contact with NaCl more frequently, and engines are often washed with local water which contains NaCl in significant amount.

Experimental investigations on the electrochemical corrosion behavior of Al and Al-Si alloys in different aqeuous media have been carried out [9]. The role of different alloying elements like Mg, Fe, Cu, Ni, Si etc. on corrosion performance of automotive alloy are being studied. However, comparatively little studies have been conducted about the role of Si on the corrosion behavior of Al-based automotive in aqueous conditions [9]. Our motive is to study the comparative effect of Si as an alloying element on the electrochemical corrosion behavior of Al-Si automotive alloy of eutectic composition in different concentrations of sodium chloride aqueous media.

## 2. Experimental procedure

A graphite crucible in a natural gas-fired pit furnace was used for melting the composing materials of the alloys. Oxidation during melting was avoided by using borax as a flux cover. For studying the effect of Si on the electrochemical properties, the following two alloys were cast. Although the motive was to cast the Alloy 1 with no amount of Si in it and Alloy 2 with around 12-13 wt% Si while keeping other elements more or less constant, trace amount of Si intruded in Alloy 1 as impurity. The chemical composition analysed by spectrochemical methods after melting shows,

Alloy 1: Al-0.2Si-2.2Cu-0.8Mg-0.2Fe

Alloy 2: Al-12.7Si-2.2Cu-0.8Mg-0.3Fe

and some Ni, Zn, Pb, Mn, Ti as trace elements, which were intruded by environment naturally. A mild steel mould of 20 mm × 200 mm × 300 mm was used for casting after preheating at 250 °C, where casting was done at 700 °C. A Shimadzu PDA 700 optical emission spectrometer was used to determine the chemical composition. The samples were homogenized at 450 °C for 12 hours and solutionized at 535 °C for 2 hours followed by quenching using an electric muffle furnace. The alloys were machined into rectagular samples of 5 mm × 5 mm × 12 mm, which was later used as working electrodes. For attaining the peak aged condition and maximum strength, the solution treated alloys were aged at 200 °C for 4 hours [10]. 320, 600, 800, 1200 and 2000 grit emery sheets were used to polish the surfaces of the samples. An optical microscope named OPTIKA was used for microstructural analysis. The experiment was conducted at 25 ± 1 °C, room temperature.

### *2.1. Potentiodynamic Polarization Technique*

The study was performed in a 100 mL standard three-electrode glass cell. As reference and counter electrodes, silver chloride (Ag/AgCl-KCl) and platinum electrodes were adopted, respectively. The experimentally machined alloys were regarded as working electrodes. The exposed surface area was only 4 × 4 $mm^2$ for each of the working electrode. The remaining surfaces were coated by PVC heat shrinkable tube. 0.1 M and 0.2 M NaCl solutions were prepared by dissolving analytical reagent grade NaCl powder into deionized water. All three electrodes were immersed in 100 mL of the NaCl solution and the electrodes were connected to a computerized CH Instruments – Electrochemical Workstation by crocodile clips. The system was kept for about 30 minutes to attain a steady state. The Tafel plots from potentiodynamic polarization analysis were recorded by changing the electrode potential automatically from -1 V to 1 V versus OCP with a scan rate of 0.5 mV $s^{-1}$. According to ASTM standard G102, the formula for determining the corrosion rate:

$$\text{Corrosion rate} = \frac{I_{\text{corr}}\, K\, EW}{\rho A} \tag{1}$$

where,

$I_{corr}$ = corrosion current, A

$K$ = constant which defines the units of corrosion rate in mmy (here, K = 3272 mm (A cm year)$^{-1}$ from ASTM Standard G 102)

$EW$ = equivalent weight, g/eq

$\rho$ = density of alloy, g cm$^{-3}$

$A$ = surface area, cm$^2$

*2.2. Electrochemical Impedance Spectroscopy (EIS) Technique*

Measuring the voltage between the working and reference electrodes yielded the values of open circuit potential. EIS approach utilized the same cell and apparatus as the potentiodynamic polarization technique. A frequency range of 100 kHz to 0.2 Hz, and a sinusoidal voltage amplitude of 5 mV were set for conducting the experimental runs. All impedance data generated from the experiments were fitted to an appropriate equivalent circuit using the program EC-Lab Analyst. The values of different circuit components and the Nyquist and Bode plots were generated. The discrepencies between the experimental and fitted data provided the goodness of fit.

## 3. Results and discussion

*3.1. Impedance measurement*

Figure 1 and Figure 2 show the Nyquist diagrams for the trace Si added and 12.7Si added experimental alloys under 0.1 M and 0.2 M NaCl solutions respectively. In order to derive the real and imaginary parts of the impedances, the capacitive-resistive semicircle model has been implemented. The Nyquist plots in Figure 1 and Figure 2 are considerably depressed, indicating that they are not ideal semicircles as suggested by electrochemical impedance spectroscopy theory. This discrepancy is explained by the double layer's non-ideal behavior as a capacitor [11].

The impedances for varying frequencies are generated by the CH Instruments – Electrochemical Workstation, which are simulated by a data analysis software, EC-lab Analyst. After modelling a few circuits for fitting the data, the best fitted one is displayed in Figure 3. $R_p$ denotes the polarization or corrosion resistance, $R_s$ denotes the ohmic solution resistance and $C_{p\text{-effective}}$ means the effective electrical double layer resistance. $R_s$ shows negligible values compared to $R_p$. Polarization resistance values are related to the working electrodes, and the solution resistance values are related to the solution used, NaCl solution in this case. According to literature, polarization resistance is inversely related to the corrosion rate of a metal, which indicates the information about the rate of reactivity of the surface with the environment [4]. Table 1 shows the test results from EIS analysis.

**Table.1.** Electrochemical impedance spectroscopy test results.

| Concentration in M | Alloy | $R_s$ in Ω | $R_p$ in kΩ | $C_{p\text{-effective}}$ in µF | OCP | Goodness of fit |
|---|---|---|---|---|---|---|
| 0.1 | 0.2Si | 42 | 10.883 | 12.91 | -0.66048 | 0.04703 |
| | 12.7Si | 66.91 | 28.502 | 11.62 | -0.63539 | 0.0257 |
| 0.2 | 0.2Si | 20.17 | 5.381 | 7.61 | -0.89805 | 0.003151 |
| | 12.7Si | 38.39 | 16.514 | 6.803 | -0.68843 | 0.003361 |

From Table 1, it is visible that the polarization resistance is higher in higher Si added alloy in both 0.1 M and 0.2 M NaCl solution, which shows a tendancy of increasing corrosion resistance in alloy with greater Si content. As around 0.8 wt% Mg is present in both alloys, added Si forms $Mg_2Si$ intermetallic, which reacts with oxygen and forms MgO and $SiO_2$ oxides as protective layers in corrosive environment of NaCl. These oxides are formed as both Mg and Si have good affinity for oxygen, which is present in

the NaCl solution. As a result, alloy with eutectic content of Si has thicker layer of oxides, which protect the surface from further corrosion [12]. Again, the value of $R_p$ is lower for 0.2 M NaCl than 0.1 M NaCl in case of both 0.2 and 12.7 wt% Si, disclosing the fact that 0.2 M NaCl acts as a destructive medium more intensively than 0.1 M NaCl. This result may be attributed to the fact that the attack by $Cl^-$ is more aggresive in higher concentrations. Again, as [$Cl^-$] increases, pitting is promoted as attack by $Cl^-$ gets dominated [13]. Moreover, The OCP value shifts towards nobler direction as Si wt% is increased. As previous studies showed that the shifting of OCP value toward positive direction indicates an increase in corrosion resistance. It is higher in higher Si added alloy, similar to previous observation [14]. It can also be observed that in 12.7Si added alloy, the $C_{p\text{-effective}}$ is lower than 0.2Si added alloy. Another interesting observation is that the ratio between the $R_p$ of 0.2Si and 12.7Si alloy for 0.1 M NaCl is 2.619 (28.502 : 10.883) and for 0.2 M NaCl is 3.069 (16.514 : 5.381), which suggests that the improvement of corrosion resistance caused by Si addition is more prominent in case of higher concentration of NaCl solution. Again, observing the similar ratios of OCP, for 0.1 M NaCl is 0.962 ((-0.63539) : (-0.66048)) and for 0.2 M NaCl is 0.767 ((-0.68843) : (-0.89805)). OCP is boosted towards positive value in 0.2 M NaCl, which supports the previous observation.

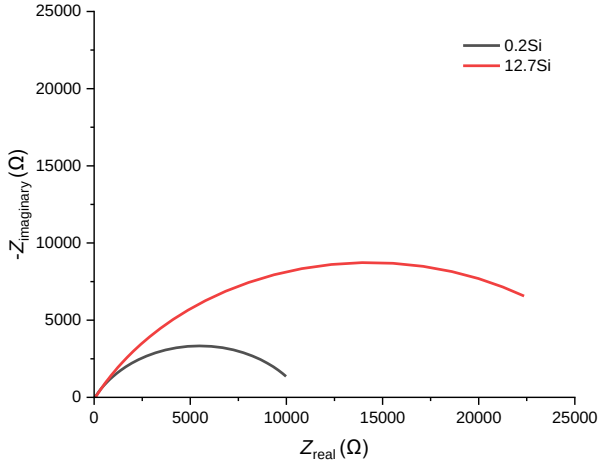


**Figure.1.** Nyquist plot for alloys with 0.2 and 12.7 wt% Si in 0.1 M NaCl

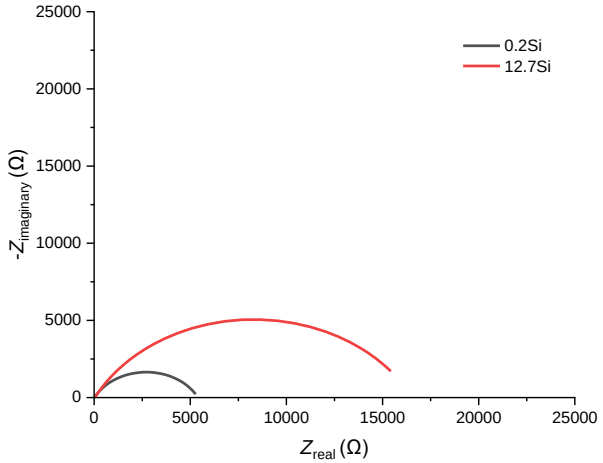


**Figure.2.** Nyquist plot for alloys with 0.2 and 12.7 wt% Si in 0.2 M NaCl

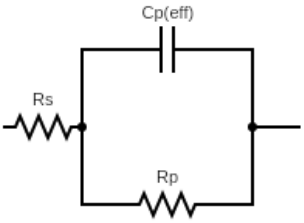


**Figure.3.** The electrical circuit to fit the EIS data

Figure 4 and 5 exhibit the Bode plots. The modulus of impedance is expressed as $Z_{\text{modulus}}$, which is defined as,

$$Z_{\text{modulus}} = \sqrt{Z_{\text{real}}{}^2 + Z_{\text{imaginary}}{}^2} \quad (2)$$

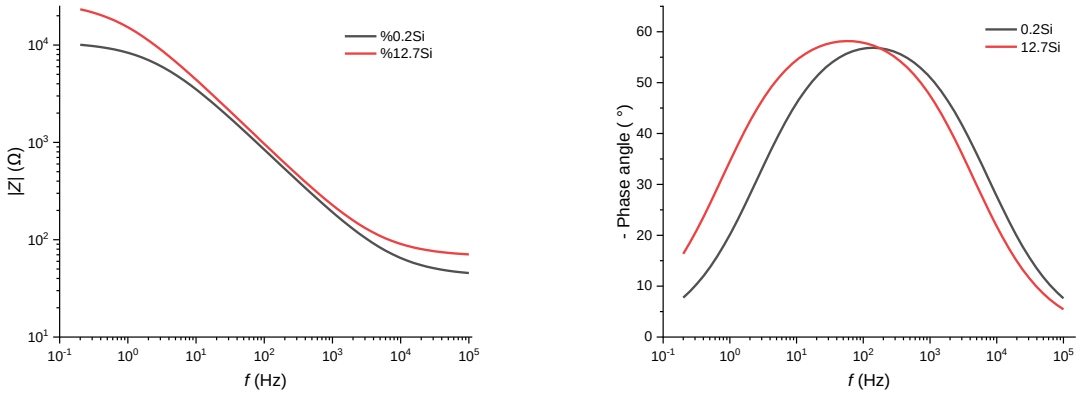


**Figure.4.** Bode plots for alloys with 0.2 and 12.7 wt% Si in 0.1 M NaCl

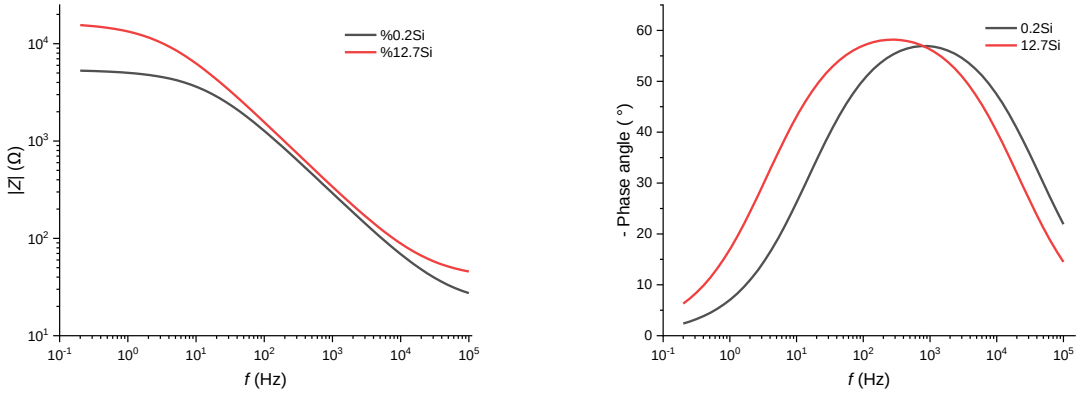


**Figure.5.** Bode plots for alloys with 0.2 and 12.7 wt% Si in 0.2 M NaCl

### *3.2. Potentiodynamic polarization analysis*

The experimental results of potentiodynamic polarization analysis are presented in Table 2. $I_{\text{corr}}$ and $E_{\text{corr}}$ represent the corrosion current and corrosion potential respectively. Corrosion rate is expressed in mmy, unit which is the corrosion loss per year in thickness.

**Table.2.** Potentiodynamic polarization test results.

| Concentration in M | Alloy | $I_{corr}$ in µA | $E_{corr}$, in V | Corrosion rate in mmy |
|---|---|---|---|---|
| 0.1 | 0.2Si | 20.178 | -597.538 | 0.8858 |
| | 12.7Si | 13.491 | -574.055 | 0.5865 |
| 0.2 | 0.2Si | 25.158 | -654.302 | 1.1667 |
| | 12.7Si | 15.898 | -630.005 | 0.6911 |

Previous studies suggest that a more positive value of corrosion potential indicates improved corrosion resistance [15]. From Table 2 it is clear that there is lower corrosion current ($I_{corr}$) and higher corrosion potential ($E_{corr}$) in higher Si added alloy, indicating higher corrosion resistance, which aligns with our previous analysis from the EIS results. Again, the corrosion rate is higher in 0.2 M NaCl than 0.1 M NaCl in case of both 0.2Si and 12.7Si added alloys, due to the more aggressivenes of $Cl^-$ in solution of higher concentration [13]. The ratio of corrosion rate between 0.2 and 12.7 wt% silicon added alloys in case of 0.2 M NaCl (0.6911 : 1.1667 = 0.592) is lesser than in case of 0.1 M NaCl (0.5865 : 0.8858 = 0.662), designating that the effect of Si on improving corrosion resistance is more pronounced in case of 0.2 M NaCl.

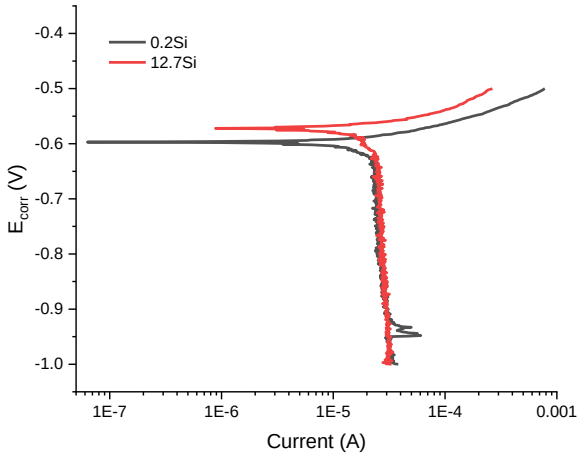


**Figure.6.** Tafel plot for alloys with 0.2 and 12.7 wt% Si in 0.1 M NaCl

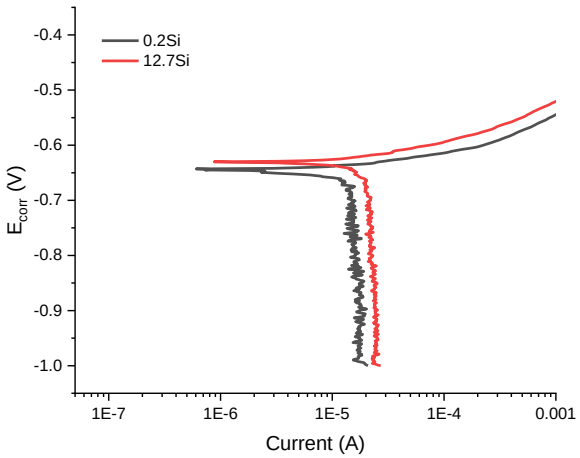


**Figure.7.** Tafel plot for alloys with 0.2 and 12.7 wt% Si in 0.2 M NaCl

*3.3. Microstructural characterization*

Figure 8 shows the optical microstructures of the surfaces of trace and 12.7 wt% Si added alloys before and after corrosion. Although too much information cannot be retrieved from this type of unetched micrographs, but an attempt for some apparent observation is taken. This type of alloy microstructure is comprised of an Al-rich dendritic matrix, eutectic Si, and various intermetallic phases. Both the alloys contain similar percentages of alloying elements except Si. It is clearly visible that the polished marks are removed after corrosion, as oxide layers are formed on the corroded surfaces. Fe and Cu with Al precipitates have a darker tone, while Si and Mg with Al precipitates have a brighter tone. Due to the variable quantities of Si in the alloys, there is a visible variation in the quantity of various tones. From the images of uncorroded surfaces, a lighter tone can be observed in case of Alloy 2, the alloy with 12.7 wt% Si, which depicts the increased amount of Si containing precipitates. Severe degradation on the surfaces of the alloys at different intensities are visible after corrosion. The optical micrographs of the alloy surfaces under 0.1 M and 0.2 M NaCl show the evidence of concentrated attacks at different locations on the surfaces. Another observation is that corrosion takes place more uniformly and with less localized pit formation on the surface of Alloy 1 than Alloy 2, as the higher amount of Si is responsible for formation fo $Mg_2Si$ particles which in turns form MgO and $SiO_2$ layers on the surface, protecting it from corrosive environment [12]. 0.2 M NaCl seems to have caused more damage on the surface than 0.1 M NaCl in case of both alloys, as higher concentration of $Cl^-$ causes more pits on the surfaces.

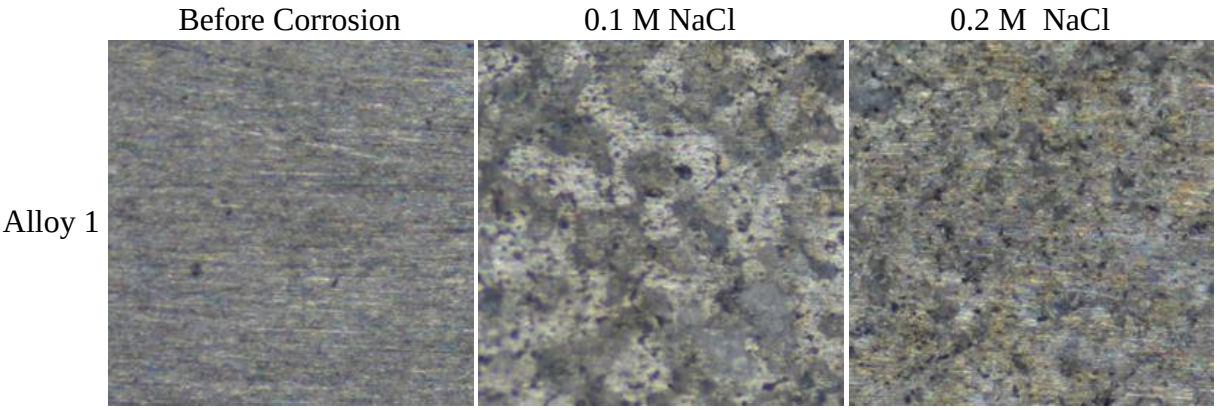

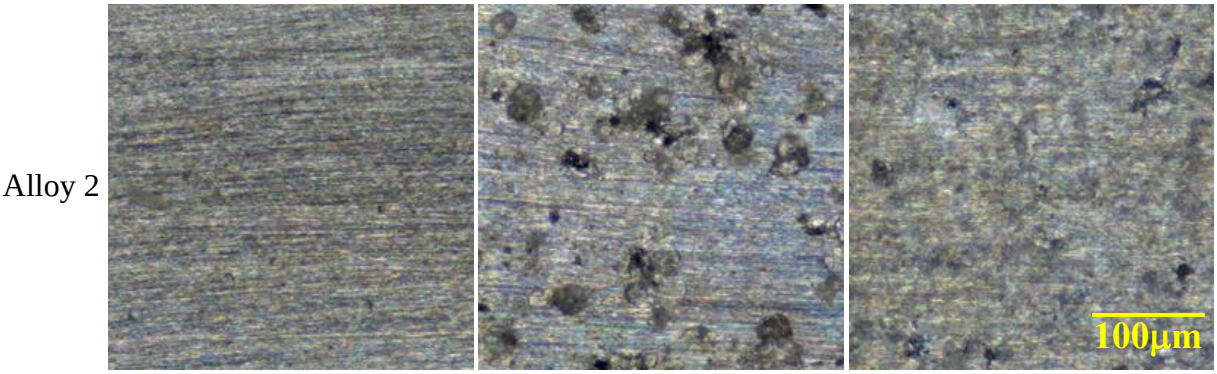


**Figure.8.** Microstructure of polished Al-Si alloys before and after corrosion at 0.1 M and 0.2 M NaCl solution.

*3.4. SEM Observation*

The SEM images are present in Figure 9, which shows the damaged surface morphology of both the experimental alloys after electrochemical corrosion in 0.1 M and 0.2 M NaCl solutions. The corrosion of intermetallic compounds on the surfaces of both the inspected alloys is evident from the images. Localized corrosion and distinct pits are also visible on the surfaces of the samples in the images. For 0.2Si added alloy it is more prominent as 12.7Si added alloy consists the higher quantity of oxide layer. On the basis of literature and previous studies, the presence of $Mg_2Si$ intermetallic may form oxides like $SiO_2$ and MgO, which protect the $Mg_2Si$ particles and reduce the galvanic coupling with the matrix. Eventually, the role of $Mg_2Si$ protects the alloy surfaces from further attack by the NaCl solution [12]. Corrosion in aluminum alloys is influenced by intermetallic particles of coarse size. The corrosive effect of these intermetallics and second-phase particles is dependent on their redox potential in relation to the matrix. Cathodes are electrochemically more noble particles, and the matrix undergoes anodic dissolution and subsequent localized corrosion. The $Al_3Fe$, $Al_2Cu$, AlCuMg, Al (Cu, Fe, Mn), AlCuFe, (Al, Cu) Mn particles are second phase particles which are cathodic to the surrounding matrix and generate localized pitting [16].

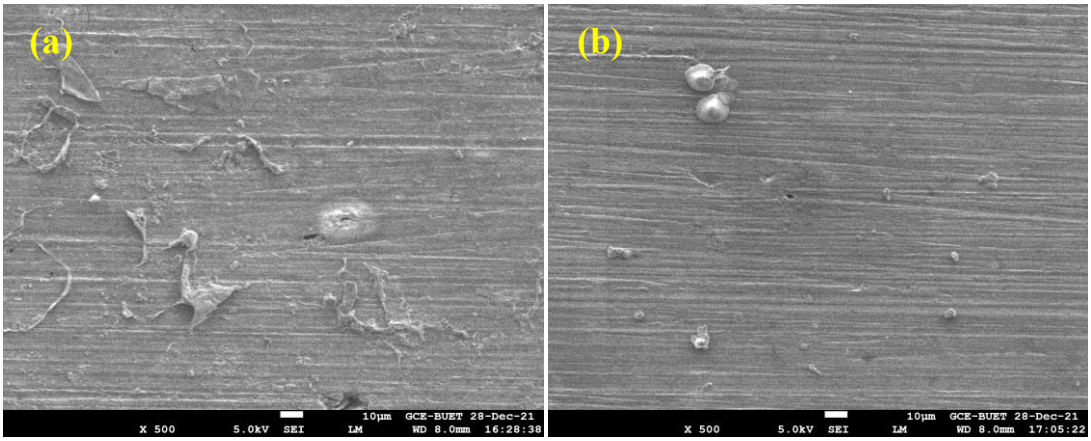

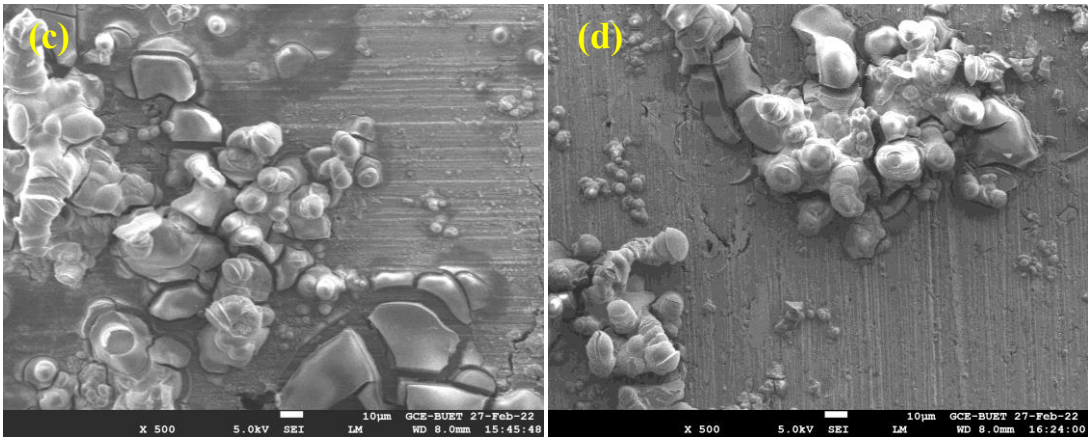


**Figure.9.** SEM images of Al-Si alloys after exposure in 0.1M and 0.2M NaCl solution (a) 0.2Si, (b) 12.7, (c) 0.2Si (d) 12.7Si.

## 4. Conclusion

This study investigated the electrochemical corrosion performance of eutectic Al-Si automotive alloy under 0.1 M and 0.2 M NaCl environment. From the study, following conclusions are emphasized:

- The alloy with higher silicon content has shown more positive values of corrosion potential and low values of corrosion current in both environments, which means lower corrosion rate in alloy with greater silicon content. $Mg_2Si$ intermetallic, which is in increased amount in the alloy with higher silicon content, forms oxide layers on the surface providing protection.
- Higher concentration of sodium chloride solution causes more deterioration to the surface quality of the alloys, as more $Cl^-$ can attack and form more pits.
- The role of silicon is more prominent under NaCl of higher concentration.
- It is observed from the microstructures and SEM images that the pitting corrosion takes place more intensively on the surfaces of the alloys under higher concentration of NaCl, which is reduced with Si addition. This reduction in pitting corrosion for Si addition is more prominent under higher concentration of NaCl solution.
- Changes in chemical composition and microstructure led to differences in electrochemical behavior. Si content determines the overall corrosion performance of the alloys, while the percentages of other alloying elements were held constant.

## Acknowledgement

The Department of Mechanical Engineering of Bangladesh University of Engineering and Technology supported this work. Thanks to Department of Chemistry for the laboratort facilities.

## References

[1] Chandel R, Sharma N and Bansal S A 2021 A review on recent developments of aluminum-based hybrid composites for automotive applications *Emergent Mater.* **4** 1243–57
[2] Al Nur M, Khan A A, Dev Sharma S and Kaiser M S 2022 Electrochemical corrosion performance of Si-doped Al-based automotive alloy in 0.1 M NaCl solution *J. Electrochem. Sci. Eng.* **12** 565–76
[3] Ma G, Qi L, Gao M and Wang Z 2022 The influence of annealing treatment on the electrocatalytic oxidation performance of Cu46Zr44·5Al7.5Gd2 amorphous alloy *Mater. Chem. Phys.* **286** 126180
[4] Hossain A, Gafur M A, Gulshan F and Kurny A S W 2014 The effects of 2wt % Cu addition on the corrosion behavior of heat treated Al-6Si-0.5Mg-2Ni alloy **8** 719–23

[5] Davis J R 1999 *Corrosion of Aluminum and Aluminum Alloys* (ASM International)
[6] Toptan F, Alves A C, Kerti I, Ariza E and Rocha L A 2013 Corrosion and tribocorrosion behaviour of Al–Si–Cu–Mg alloy and its composites reinforced with B4C particles in 0.05M NaCl solution *Wear* **306** 27–35
[7] Cardenas Almena M D, Lucio Esperilla O, Martin Manzanero F, Murillo Duarte Y, Quintero Toscano L C and Wolff G 2012 Internal diesel injector deposits: sodium carboxylates of C12 succinic acids and C16 and C18 fatty acids
[8] Barker J, Cook S and Richards P 2013 Sodium contamination of diesel fuel, its interaction with fuel additives and the resultant effects on filter plugging and injector fouling *SAE Int. J. Fuels Lubr.* **6** 2013-01–2687
[9] Salih S A, Gad-Allah A G, Mazhar A A and Tammam R H 2001 Effect of silicon alloying addition on the corrosion behaviour of aluminium in some aqueous media *J. Appl. Electrochem.* **31** 1103–8
[10] Kaiser M S, Basher M R and Kurny A S W 2012 Effect of scandium on microstructure and mechanical properties of cast Al-Si-Mg alloy *J. Mater. Eng. Perform.* **21** 1504–8
[11] Amira W A W E, Rahim A A, Osman H, Awang K and Raja P B 2011 Corrosion inhibition of mild steel in 1 M HCl solution by Xylopia ferruginea leaves from different extract and partitions *Int. J. Electrochem. Sci.* **6** 2998–3016
[12] Escalera-Lozano R, Pech-Canul M I, Pech-Canul M A, Montoya-Davila M and Uribe-Salas A 2010 The role of Mg2Si in the corrosion behavior of Al-Si-Mg alloys for pressureless infiltration *Open Corros. J.* **3** 73–9
[13] Mazhar A A, Arab S T and Noor E A 2001 The role of chloride ions and pH in the corrosion and pitting of Al-Si alloys *J. Appl. Electrochem.* **31** 1131–40
[14] Choudhary S, Garg A and Mondal K 2016 Relation between open circuit potential and polarization resistance with rust and corrosion monitoring of mild steel *J. Mater. Eng. Perform.* **25** 2969–76
[15] Abdallah M, Kamar E M, Eid S and El-Etre A Y 2016 Animal glue as green inhibitor for corrosion of aluminum and aluminum-silicon alloys in sodium hydroxide solutions *J. Mol. Liq.* **220** 755–61
[16] Szklarska-Smialowska Z 1999 Pitting corrosion of aluminum *Corros. Sci.* **41** 1743–67